Andean Geology 51 (3): 547-558. September, 2024
doi: 10.5027/andgeoV51n3-3736

Andean Geology
www.andeangeology.cl

GEOLOGICAL NOTE

The subaqueous felsic volcanism from the Upper Member of the Cordón de Lila Complex, Antofagasta region, northern Chile

Hans Niemeyer*

* *Departamento de Ciencias Geológicas, Universidad Católica del Norte, Angamos 0610, Antofagasta, Chile.*
hansn@ucn.cl

ABSTRACT. This contribution presents the study of an Ordovician subaqueous felsic succession, formed by the ~400 m-thick Upper Member of the Cordón de Lila Complex (CISL), northern Chile. From bottom to top, the succession starts with two dacitic sills that intruded into the sediments of the lowermost part of the Upper Member. Then, it is followed by a thick sedimentary deposit, two rhyolitic lavas, a volcanoclastic felsic breccia with pyroclastic clasts, and ends with a red rhyolitic lava. The first rhyolitic lava shows centimetric to metric folds with a north-northwestern vergence, evidence of flow in that direction. In the volcanoclastic breccia, an abundant pumice-and-fiamme-rich green matrix wraps around lithic clasts, giving the rock an eutaxitic texture at the outcrop scale. This matrix and texture evidence is characteristic of hot pyroclastic flows deposited under subaqueous conditions. The described section of the breccia is formed by four coarsening-up sequences, reflecting respectively four pulses of building up energy. The lack of internal erosional features points to a single and continuous explosive eruption. An accidental granite clast in the upper part of the breccia suggests a connection with a granitic body, possibly the Pingo-Pingo monzogranite. The geochemical character of the felsic succession is calc-alkaline. The tectonic setting diagram shows a within-plate setting for the succession. This suggests a shift from the arc position inferred for the Lower Member of the CISL to a forearc continental setting for the Upper Member of the CISL.

Keywords: Subaqueous felsic succession, Continental forearc, Ordovician.

RESUMEN. El volcanismo subacuático del Miembro Superior del Complejo Cordón de Lila, región de Antofagasta, norte de Chile. Este trabajo presenta una sucesión subacuática félsica ordovícica, formada por el miembro superior del Complejo ígneo-sedimentario del Cordón de Lila (CISL), el que posee un espesor de ~400 m. De base a techo, la sucesión incluye dos filones-manto dacíticos, intruidos en sedimentos de la parte inferior de dicho miembro. Luego presenta un intervalo de sedimentitas, dos lavas riolíticas y una brecha volcanoclástica félsica con clastos piroclásticos. La secuencia finaliza con una lava riolítica rojiza. El primer flujo de lava riolítica contiene pliegues métricos a centimétricos con vergencia hacia el nornoroeste, lo que indica un flujo en ese sentido. La brecha tiene una abundante matriz verdosa formada por fiamme y pómez soldadas que rodean a los clastos líticos, y otorgan a la brecha una conspicua textura eutaxítica. El tipo de matriz y la textura observadas son características de flujos piroclásticos calientes depositados en ambientes submarinos. La sección descrita de la brecha puede dividirse en cuatro secuencias granocrecientes, las cuales reflejan, respectivamente, cuatro pulsos de energía creciente. La ausencia de discontinuidades internas apunta a una única erupción explosiva. La presencia de un clasto accidental de granito en la brecha sugiere una conexión con un intrusivo granítico en profundidad, posiblemente el monzogranito Pingo-Pingo. La afinidad geoquímica de la sucesión es calcoalcalina. En el diagrama de ambientes tectónicos, las volcanitas del miembro superior caen dentro del campo de intraplaca. Esto sugiere un cambio desde un ambiente de arco volcánico para el miembro inferior del CISL a una posición de antearco continental para el miembro superior del CISL.

Palabras clave: Sucesión félsica subacuática, Antearco continental, Ordovícico.

1. Introduction

Subaqueous eruptions are the most abundant on Earth (McPhie *et al.*, 1993; Deligne and Sirgurdsson, 2015). Nevertheless, direct felsic subaqueous eruption observations at modern volcanoes remain limited. A simple and still useful approach is the observation and description of felsic associations within ancient volcano-sedimentary subaqueous sequences. This may supply important clues for understanding the subaqueous behavior of felsic volcanism.

The aim of this paper is to study an ancient subaqueous felsic succession, composed of rhyolitic lava flows in its lower part and a volcanoclastic felsic breccia in its upper part. Pyroclastic flows and their subsequent deposits are primary products of explosive subaqueous magmatic eruptions (Stix, 1991; White *et al.*, 2015a). Explosive eruptions capable of generating primary pyroclastic flows can be produced in relatively deep subaqueous settings, and these flows have been observed to maintain their integrity underwater (McBirney, 1963; Newland *et al.*, 2022). The subaqueous environment can also promote welding and compaction more easily compared to subaerial environments (Sparks *et al.*, 1980; Stix, 1991; Kokelaar and Busby, 1992).

2. Geological setting

The Cordón de Lila, in northern Chile (Fig. 1), exposes the Lower to Middle Ordovician Cordón de Lila Complex or CISL (Complejo ígneo-sedimentario del Cordón de Lila; Niemeyer, 1989). The CISL is formed by a ~2,500 m-thick Lower Member of pillowed basalts, andesites and turbidites and a 400 m-thick Upper Member of rhyolite lavas and a volcanoclastic felsic breccia with occasional sedimentary levels. The Lower Member has been intensively studied and a tholeiitic chemical character was established for their basalts and andesites (Damm *et al.*, 1990; Zimmermann *et al.*, 2010). The CISL developed in the ~NW-oriented continental Famatinian magmatic arc in the western border of Gondwana (Niemeyer *et al.*, 2018; Rapela *et al.*, 2018). The Upper Member of the CISL remains unknown in their stratigraphic, petrographic and geochemical characteristics. This member crops out in the western part of the Cordón de Lila range (Fig. 2). A stratigraphic section of the Upper Member was studied in the Quebrada del Viento creek (Fig. 3). The switch between the pillowed basalts of the Lower Member to the Upper Member is evidenced by two ~N-S-oriented dacitic sills that intruded sediments. Then, it is covered by

FIG. 1. Location of the Cordón de Lila range in the Antofagasta region, northern Chile.

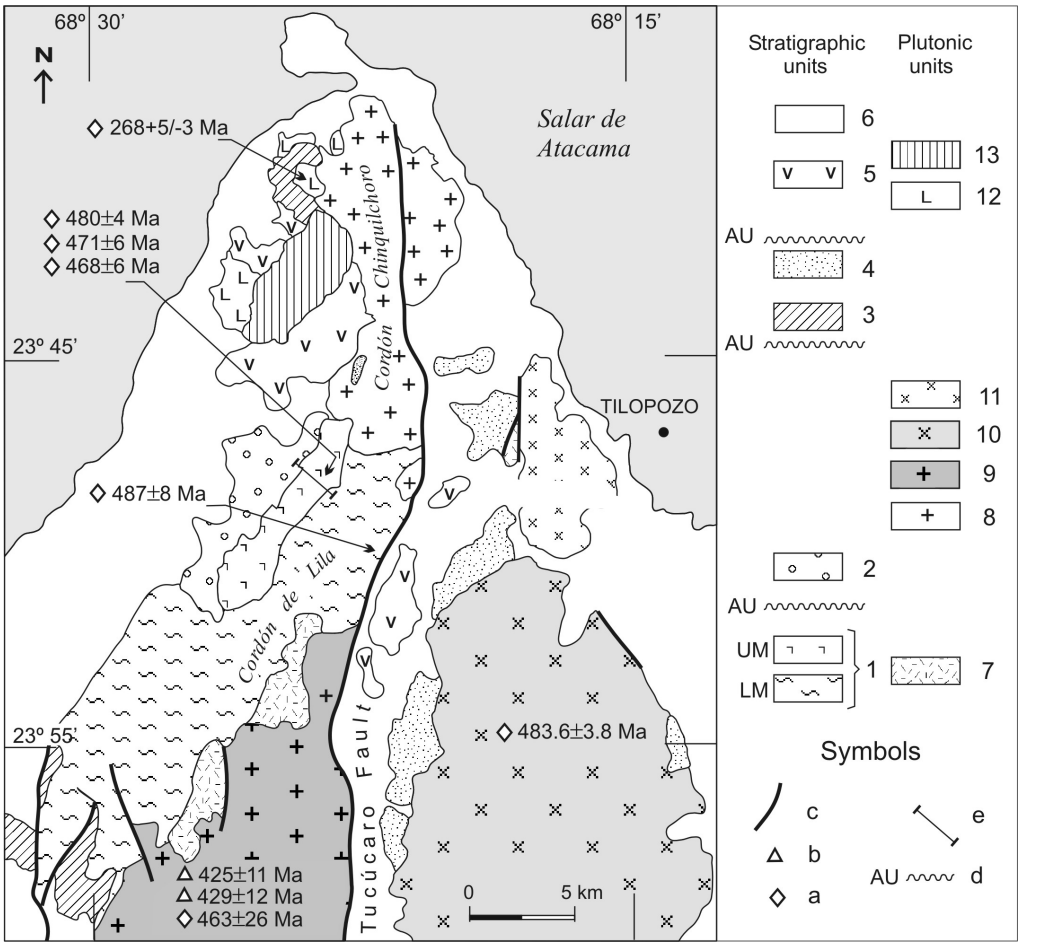

FIG. 2. Geology of the Cordón de Lila (see location in figure 1). **1**. Cordón de Lila Complex (CISL, Lower to Middle Ordovician). **LM**: Lower Member, subaqueous pillowed basalts and turbidites. **UM**: Upper Member, subaqueous rhyolite lavas and a volcanoclastic felsic breccia. **2**. Quebrada Grande Formation: marine conglomerates, sandstones and siltstones (Middle Ordovician). **3**. Quebrada Ancha Formation: marine conglomerates and sandstones (Silurian). **4**. Lila Formation: marine to continental sandstones and conglomerates (Devonian). **5**. Cerro Negro Strata: continental conglomerates, andesites and dacites (Permian). **6**. Alluvial continental deposits and ignimbrites (Pliocene to Holocene). **7**. Cerro Alto diorite (Lower Ordovician). **8**. Cerro Lila granodiorite (Lower to Middle Ordovician). **9**. Pingo-Pingo monzogranite (Lower Ordovician). **10**. Tambillo monzogranite (Lower Ordovician). **11**. Tucúcaro monzogranite (Lower Ordovician). **12**. Chinquilchoro monzodiorite (Permian). **13**. Quebrada del Gancho monzogranite (Permian-Triassic). Age data: **a**. U-Pb in zircons, **b**. K-Ar in biotite or hornblende. Other symbols: **c**. Fault, **d**. Angular unconformity (AU), **e**. Stratigraphic section at the Quebrada del Viento creek.

a thick sedimentary unit, two rhyolitic lavas, and a volcanoclastic matrix-supported breccia with green welded pyroclastic clasts. The succession ends with a red rhyolitic lava.

3. Methods

The associated lineations with centimetric folds in the rhyolitic lava flows were measured and projected in the horizontal plane with a Brunton compass. The axial planes of the flow-induced folds were estimated by means of one axis directly measured and another axis constructed by means of measurements in their flanks with the Brunton compass. To project these measurements, the Wulff stereographic net was employed. The fold vergence was determined by tracing a perpendicular line to the strike of the fold axial plane.

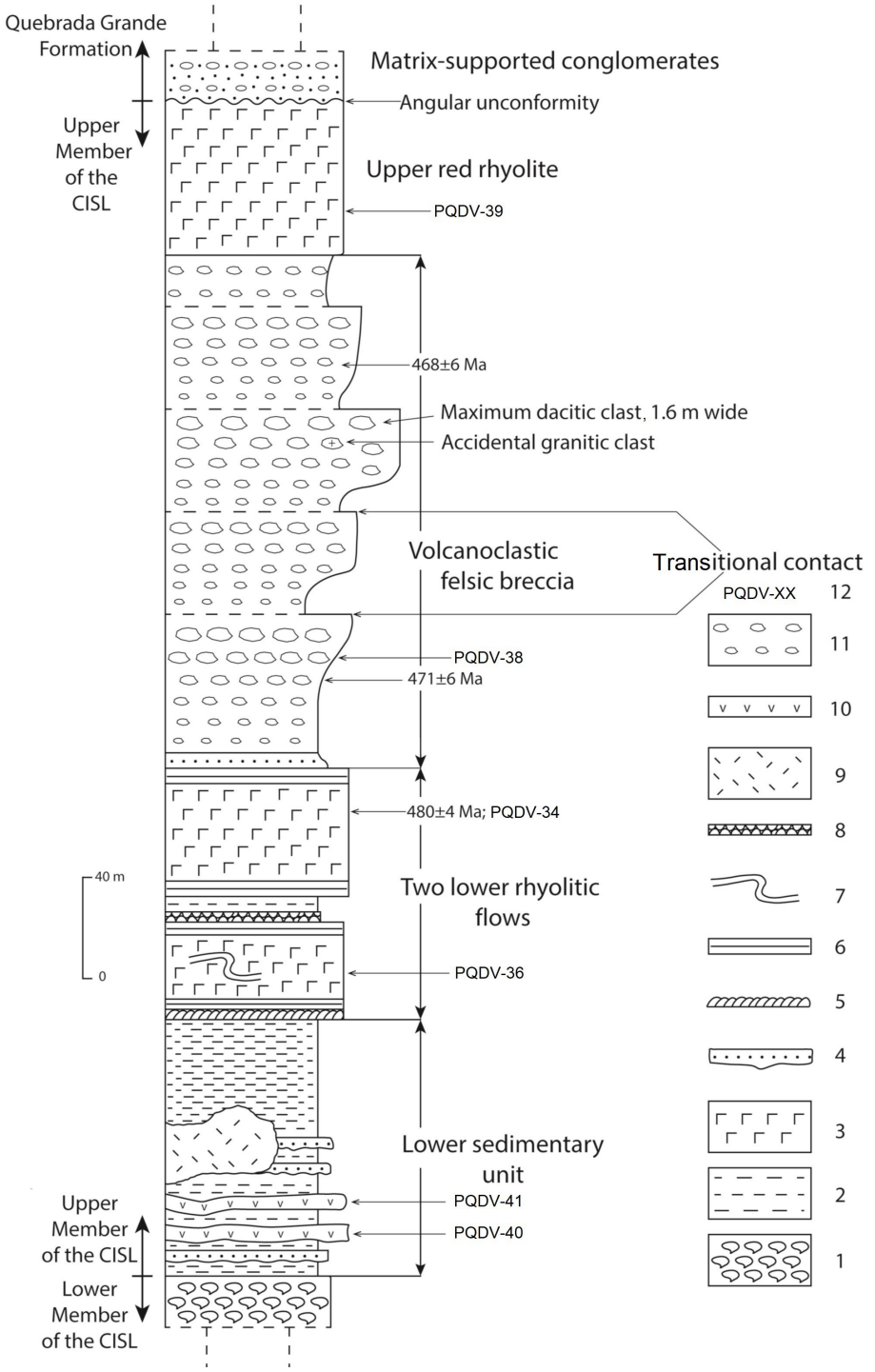

FIG. 3. Idealized stratigraphic section of the Upper Member of the Cordón de Lila Complex at the Quebrada del Viento creek (see location in figure 2). **1**. Basaltic pillow lava. **2**. Shale. **3**. Rhyolite. **4**. Turbidite. **5**. Centimetric asymmetric folds. **6**. Flow banding. **7**. Metric asymmetric flow fold. **8**. Hyaloclastite. **9**. Basaltic intrusion. **10**. Dacitic sills. **11**. Volcanoclastic felsic breccia. **12**. Chemically analyzed samples.

For the geochemical data, major elements were determined through X-Ray spectrometry in powdered samples in a Siemens SRS-3000. Trace elements were determined by inductively coupled plasma-atomic emission spectrometry (ICP-AES). The fiamme mineralogical composition was determined by X-Ray powder diffraction (XRD) in a Siemens D5000. The chemical analyses were performed in the Geochemical Laboratory of the Departamento de Ciencias Geológicas, Universidad Católica del Norte at Antofagasta, Chile.

Volcanic and volcanoclastic rocks were described according to the Cas and Wright (1987), and McPhie *et al.* (1993) terminology. UTM coordinates of all analyzed samples are: PQDV-34: 7,365,151 N, 559,409 E; PQDV-36: 7,365,103 N, 559,555 E; PQDV-38: 7,365,225 N, 559,243 E; PQDV-39: 7,365,368 N, 559,045 E; PQDV-40: 7,364,957 N, 559,853 E; and PQDV-41: 7,364,971 N, 559,749 E. The location of these samples in an idealized stratigraphic column is shown in figure 3.

4. Age and contact relationships

Two zircon LA-ICP-MS U-Pb ages of 468±6 and 471±6 Ma were obtained by Zimmermann *et al*. (2010) on dacitic clasts of the volcanoclastic felsic breccia of the Upper Member. On the other side, Pankhurst *et al.* (2016) reported one magmatic SHRIMP U-Pb age in zircons for the second rhyolitic lava flow of 480±4 Ma (see locations in figures 2 and 3). The Upper Member is overlain by means of an angular unconformity by the Dapingian-early Darriwilian conglomerates of the Quebrada Grande Formation (Benedetto *et al.*, 2007). All these ages are consistent between them and give a Lower to Middle Ordovician age for the Upper Member of the CISL.

5. Magmatic and volcanic units of the Upper Member of the CISL

The different magmatic, volcanic, and volcanoclastic units of the Upper Member of the CISL are described below. An idealized stratigraphic section is shown in figure 3.

6. Dacitic sills

These are two 2-10 m-thick tabular sills intruding sedimentary rocks in the lowermost part of the Upper Member of the CISL. These sills are composed of an aphyric rock formed by a felsitic matrix and micro-phenocrysts of plagioclase. The composition of the sills is dacitic.

7. Rhyolitic lava flows

In the literature, rhyolitic lava flows have the following characteristics: conformable with respect to the bedding, no crosscutting relationships, quenched margins, internally coherent structure, uniformly porphyritic texture, and absence of zoning (*e.g.,* Cas, 1978). These lava flows are non-vesiculated, microcrystalline, and flow-banded at their base and top.

The two rhyolitic lava flows at the base of the sequence have 2-5 mm-sized phenocrysts of automorphic to sub-automorphic feldspar and quartz immersed in a felsitic flow-banded matrix. Feldspar corresponds to plagioclase and gives the rock a porphyritic texture. Scarce, altered micro-phenocrysts of possible amphibole were also observed. Quartz shows typical embayment texture. In the matrix, small irregular patches of calcite are present, some altering plagioclase phenocrysts.

The red rhyolite lava flow at the top of the sequence is composed of embayed quartz and sub-automorphic plagioclase phenocrysts, which together with biotite are embedded in a very fine-grained devitrified groundmass composed of felsic minerals, carbonate and opaque minerals.

The lowermost first rhyolitic lava flow shows noteworthy corrugations (Fig. 4A) at its base that are associated with centimetric folds (Fig 4B) whose vergence marks a north-northwest direction of flow (Fig. 5A). This unit also has in its middle part a metric flow-fold with a curved hinge (Fig. 4C) and ~NW vergence (Fig.5B). At the top of the first rhyolitic lava, it can be observed the passage to a 2-3 m-thick fine-grained white hyaloclastite.

In the upper second rhyolitic lava, evidence of flow banding is present only at the base and top. A turbiditic unit marks the top of this lava flow and separates it from the volcanoclastic felsic breccia.

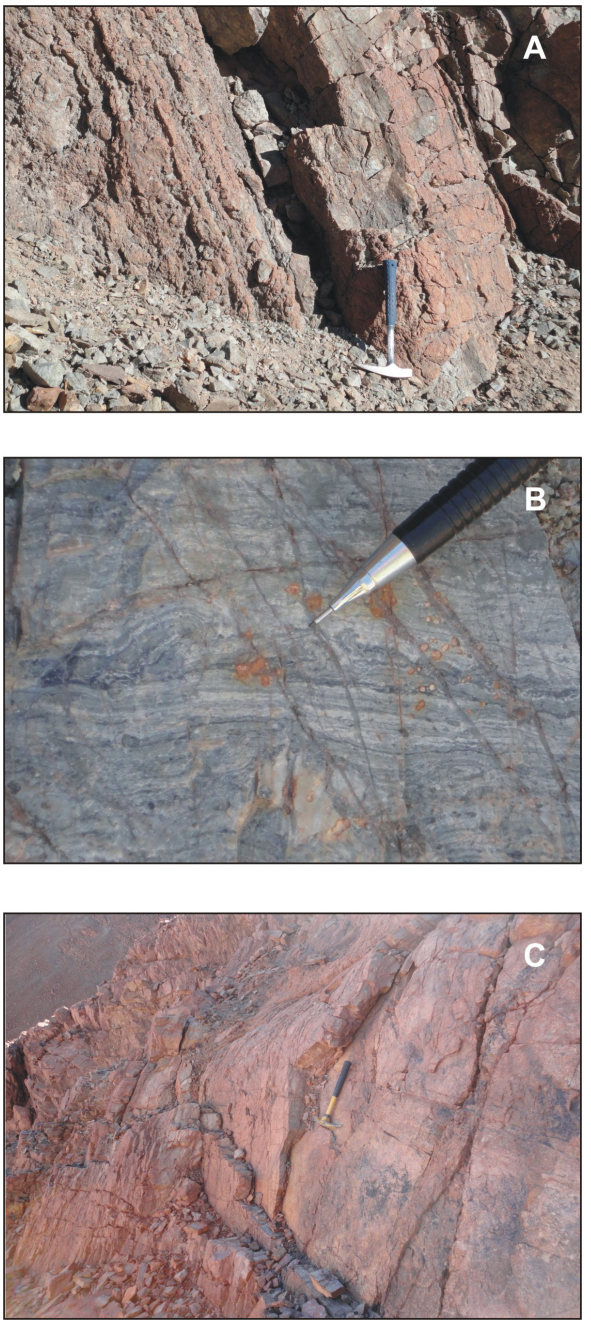

FIG. 4. Folds in the first rhyolitic lava flow in the Upper Member of the CISL. **A**. Corrugations at the base. **B**. Centimetric fold associated with corrugations. **C**. Metric fold in the middle part of this unit.

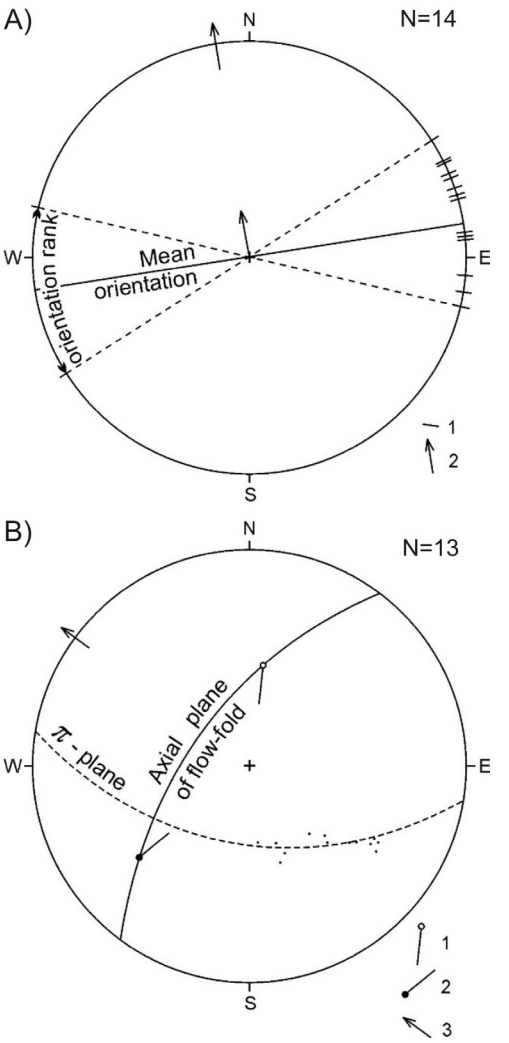

FIG. 5. Stereograms of flow folds in the first rhyolitic lava. **A**. Mean orientation of centimetric flow lines at the base: **1**. Axes of centimetric flow folds. **2**. Vergence direction based on the mean calculated orientation. **B**. Metric flow fold data: **1**. Constructed fold axis. **2**. Measured flow axis. **3**. Vergence direction perpendicular to the constructed axial plane. Wulff net projection.

8. Volcanoclastic felsic breccia

The volcanoclastic felsic breccia consists of an abundant green, pumice-and-fiamme-rich matrix (60%) wrapped around 5-40 cm-long, rhyolitic banded polyhedral fragments (40%) (Fig. 6A and B). The wrapping of the fiamme around the clasts gives the rock an eutaxitic structure at the outcrop scale (Fig. 6C). Fiamme aspect ratios vary between 5:1 and 16:1 (Fig. 6D). They are aligned parallel to internal bedding and contain quartz phenocrysts (Fig. 6E). A deep green color is typical of the fiamme and they show evidence of silicification processes with quartz, albite, muscovite, celadonite, orthoclase and calcite, being the celadonite also responsible for the green color of the breccia. Ductile folding in some fiamme reflects a plastic deformation during deposition (Fig. 6F).

The stratigraphic section of the volcanoclastic breccia can be divided into four coarsening-up sequences (Fig. 3). These sequences show transitional contacts between them and reflect respectively four pulses of building-up energy. From bottom to top, the third of these sequences is indicative of the highest energy due to the presence of large (up to 1.6 m-wide) clasts (Fig. 3). This third sequence also includes an accidental granitic clast (Fig. 7).

The presence of turbiditic beds at the base of this unit, together with shale beds observed elsewhere, suggest that the whole Upper Member of the CISL was deposited under relatively deep subaqueous conditions.

9. Chemical composition

The chemical compositions of the analyzed samples that compose the Upper section of the CISL are shown in tables 1 and 2 (see stratigraphic locations in figure 3). According to the TAS diagram, all samples correspond to rhyolites excepting samples 40 and 41 which are from the dacitic sills (Fig. 8A). In the AFM diagram, all samples plot in the calc-alkaline field (Fig. 8B), in contrast with the tholeiitic character of the Lower Member (Damm *et al*., 1990). In the tectonic discrimination diagram for granites, all samples fall in the within-plate field (Fig. 8C), suggesting a shift in the magmatic source from the arc position inferred for the Lower Member to a forearc continental setting for the Upper Member (*e.g.,* Pearce, 1996) (Fig. 9).

10. Discussion

Pyroclastic flows are primary products of explosive subaqueous hot magmatic eruptions due to the presence of turbidity currents (Stix, 1991; Kokelaar and Busby, 1992; Wright *et al*., 2003; White *et al.*, 2015a). Subaqueous flow of a gas-supported density current is controlled by the excess density of the current relative to water, and it requires a very high particle concentration to overcome the low density of the gas phase (White, 2000; Moorhouse and White, 2016). The generation of fiamme is interpreted as the result from flattening and sintering of rhyolitic banded juveniles in a pyroclastic flow during welding and implies that it occurred by post-depositional compaction within the still hot deposit (Gifkins *et al*., 2005; Bull and McPhie, 2007). These subaqueous flows can be emplaced at high temperature under deep water conditions due to the high solubility of steam in rhyolitic glass at relatively high pressures (Sparks *et al*., 1980; White, 2000). There can be a substantial reduction in glass viscosity after emplacement at deep water depths. Indeed, deep underwater conditions make the welding of the matrix of a felsitic hot pyroclastic flow deposit easy (Sparks *et al.*, 1980; Stix, 1991). Another evidence of a subaqueous environment is the presence of hyaloclastites on top of the first rhyolitic lava flow, which suggests a high degree of undercooling (Shelley, 1992; White *et al.*, 2015b).

The stratigraphic section of the volcanoclastic breccia can be assigned to a single and continuous explosive eruption. The section was divided here into four coarsening-up sequences that reflect respectively four pulses. The lack of internal discontinuities gives additional support to the field observation of a single explosive eruption (*e.g*., Furukawa *et al*., 2014). The accidental granite clast in the upper part of the breccia suggests that it could be a rip-up clast of a granitic body, located in the wall of the sustained explosive source of the breccia. This body could be the Pingo-Pingo monzogranite (Fig. 9).

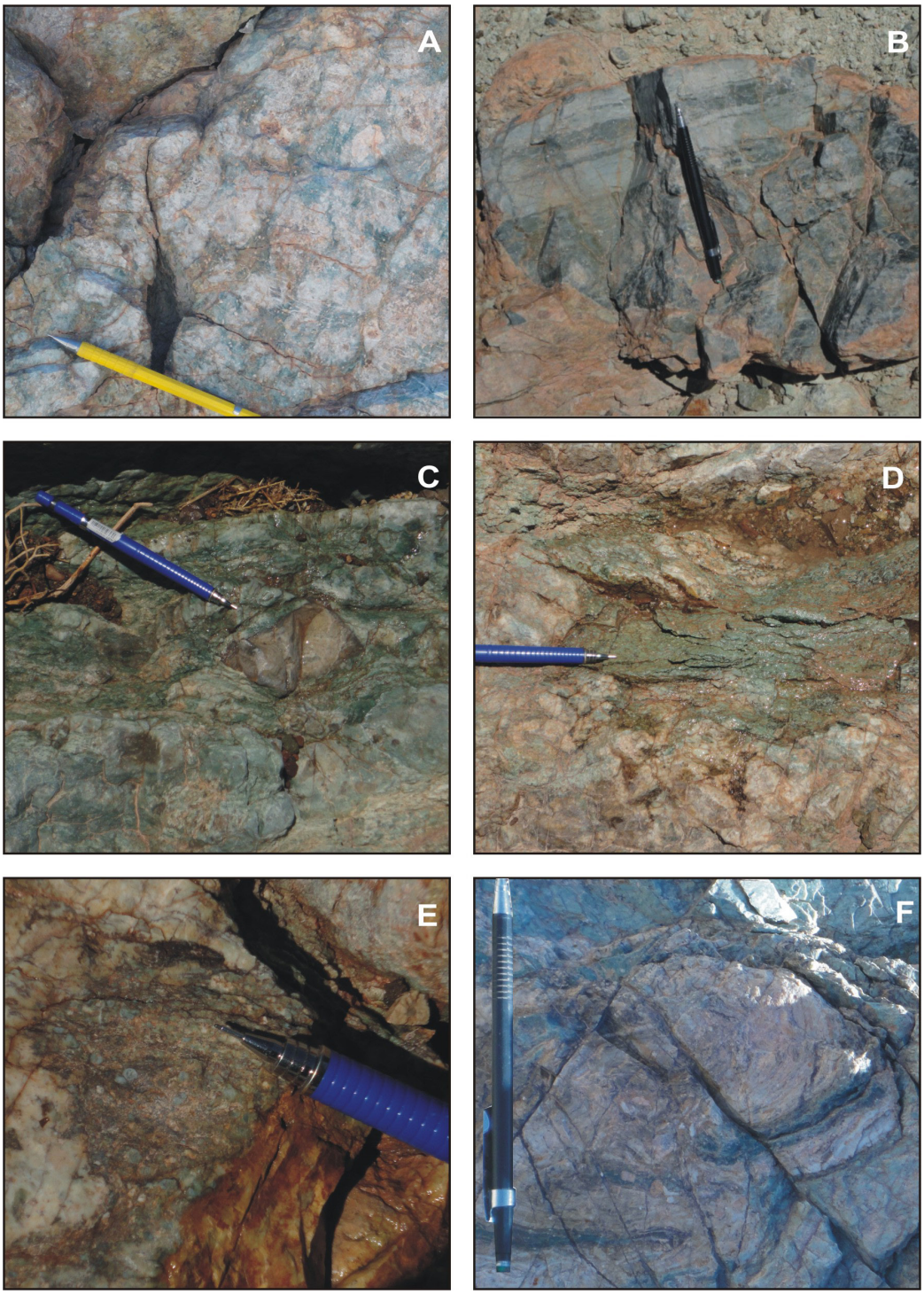

FIG. 6. Volcanoclastic felsic breccia in the Upper Member of the CISL. **A**. General look of the breccia at outcrop scale. **B**. Banded, cm-long rhyolitic clast. **C**. Eutaxitic texture shown in the breccia given by wrapping around a lithic clast. **D**. Elongated green fiamme. **E**. Quartz phenocrysts in one of the fiamme. **F**. A long fiamme strip forming a ductile fold, indicative of plastic deformation during deposition.

FIG. 7. Accidental granitic clast from the third level of the volcanoclastic felsic breccia (see stratigraphic location in figure 3).

TABLE 1. CHEMICAL ANALYSES OF MAJOR ELEMENTS, UPPER MEMBER OF THE CISL.

Sample	SiO_2 (wt%)	Al_2O_3 (wt%)	Fe_2O_3 (wt%)	FeO (wt%)	CaO (wt%)	MgO (wt%)	K_2O (wt%)	Na_2O (wt%)	TiO_2 (wt%)	P_2O_5 (wt%)	MnO (wt%)	SO_3 (wt%)	LOI (wt%)	H_2O^- (wt%)
PQDV-34	81.60	9.82	0.49	0.27	0.43	0.35	0.08	6.08	0.05	bdl	0.03	0.02	0.70	0.06
PQDV-36	81.09	8.98	0.35	0.32	0.15	0.22	6.44	1.36	0.05	bdl	0.03	0.04	0.91	0.07
PQDV-38	78.15	11.15	0.21	0.73	0.30	0.46	5.19	2.42	0.13	bdl	0.02	0.01	1.00	0.16
PQDV-39	77.50	10.96	0.76	0.55	0.55	0.78	4.41	2.83	0.19	0.03	0.02	0.01	1.23	0.14
PQDV-40	67.97	13.15	3.27	1.86	0.39	3.56	2.08	4.75	0.38	0.08	0.09	0.04	2.13	0.06
PQDV-41	68.47	14.23	1.49	1.10	0.31	1.52	9.06	1.75	0.36	0.07	0.06	0.05	1.37	0.06

LOI: Lost on ignition; **bdl**: below detection limit.

TABLE 2. CHEMICAL ANALYSES OF TRACE ELEMENTS, UPPER MEMBER OF THE CISL.

Sample	Hf (mg/kg)	Nb (mg/kg)	Rb (mg/kg)	Ta (mg/kg)	Y (mg/kg)	Zr (mg/kg)	Yb (mg/kg)
PQDV-34	8.3	23	96	17	7	45	55
PQDV-36	8.5	25	418	21	28	57	39
PQDV-38	38	23	274	18	16	79	49
PQDV-39	39	19	128	16	6	80	92

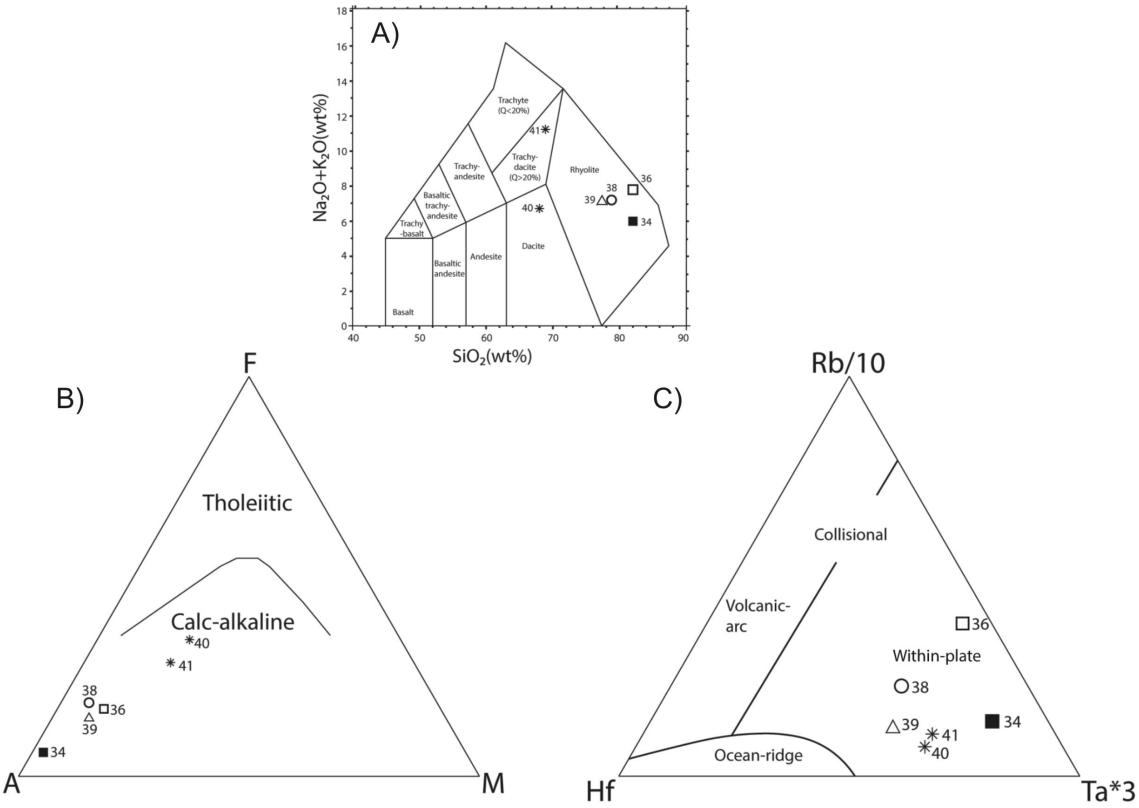

FIG. 8. Chemical composition of the samples of the Upper Member of the CISL (see stratigraphic location in figure 3). **A**. TAS (total alkali versus silica) diagram (after Middlemost, 1994). **B**. AFM (Alkali, Fe, Mg), ternary diagram that discriminates between tholeiitic and calc-alkaline rocks (curve after Irvine and Baragar, 1971). **C**. Rb-Hf-Ta tectonic discrimination diagram for granites (after Pearce *et al.*, 1984), used in this study for rhyolitic rocks. Major and trace element data are shown in tables 1 and 2, respectively.

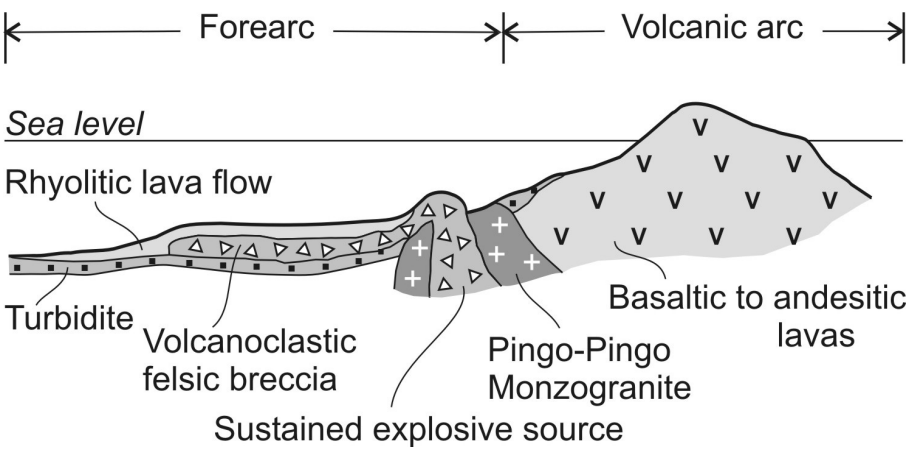

FIG. 9. Paleogeographic sketch showing the sustained explosive source of the volcanoclastic felsic breccia in a forearc position. A turbidite flow coming from the volcanic arc and a rhyolitic lava flow are also shown.

11. Conclusions

This contribution provides new insights regarding the Upper Member of the Cordón de Lila Complex. Evidence is put forth here in favor of the underwater emplacement of the whole sequence. In one of the rhyolitic flows at the base of the sequence, the occurrence of centimetric to metric folds implies that the lava had a plastic behavior during emplacement. The volcanoclastic felsic breccia that makes up the upper half of the section indicates a single explosive eruption with four pulses, of which the third was the most energetic. In this third pulse, the presence of a granitic accidental clast could be indicative that the eruption affected part of the Pingo-Pingo monzogranite. The geochemical character of the rocks of the Upper Member represents a drastic switch between the tholeiitic character of the basalts of the Lower Member of the CISL and the calc-alkaline character of the dacites and rhyolites of the Upper Member. Finally, a within-plate setting for the Upper Member rocks suggests a shift in the magmatic source from an arc (Lower Member) to a forearc (Upper Member) position.

Aknowledments

Thank is given to N. Guerra for the chemical analyses. S. Niemeyer helped in the configuration of the tables of chemical elements. A.M. Combina and C. Cisterna helped reviewing this contribution. D. Bertin, the editor, substantially improved the final version of this paper. L. Jofré designed the figures of this paper

References

Benedetto, J.L.; Niemeyer, H.; González, J.; Brussa, E.D. 2007. First record of Ordovician brachiopods and graptolites from Cordón de Lila (Puna de Atacama), Norte de Chile. Ameghiniana 45 (1): 3-12.

Bull, K.F.; McPhie, J. 2007. Fiamme textures in volcanic successions: Flaming issues of definition and interpretation. Journal of Volcanology and Geothermal Research 164 (4): 205-216. https://doi.org/10.1016/j.jvolgeores.2007.05.005

Cas, R. 1978. Silicic lavas in Paleozoic flyschlike deposits in New South Wales, Australia: Behavior of deep subaqueous silicic flows. Geological Society of America Bulletin 89 (12): 1708-1714. https://doi.org/10.1130/0016-7606(1978)89%3C1708:SLIPFD%3E2.0.CO;2

Cas, R.; Wright, J.V. 1987. Volcanic successions: modern and ancient. A geological approach to processes, products and successions. Allen and Unwin: 518 p. London, Boston, Sydney, Wellington.

Damm, K.W.; Pichowiak, S.; Harmon, R.S.; Todt, W.; Kelley, S.; Omarini, R.; Niemeyer, H. 1990. Pre-Mesozoic evolution of the central Andes: the basement revisited. In Plutonism from Antarctica to Alaska (Kay, S.M.; Rapela, C.W.; editors). Geological Society of America, Special Paper 241: 101-126. Boulder. https://doi.org/10.1130/SPE241-p101

Deligne, N.I.; Sigurdsson, H. 2015. Global rates of volcanism and volcanic episodes. The Encyclopedia of Volcanoes (Second Edition): 265-272. https://doi.org/10.1016/B978-0-12-385938-9.00014-6

Furukawa, K.; Uno, K.; Shinmura, T.; Miyoshi, M.; Kanamaru, T.; Inokuchi, H. 2014. Origin and mode of emplacement of lithic-rich breccias at Aso Volcano, Japan: Geological, paleomagnetic, and petrological reconstruction. Journal of Volcanology and Geothermal Research 276: 22-31. https://doi.org/10.1016/j.jvolgeores.2014.02.010

Gifkins, C.C.; Allen, R.L.; McPhie, J. 2005. Apparent welding textures in altered pumice-rich rocks. Journal of Volcanology and Geothermal Research 142 (1-2): 29-47. https://doi.org/10.1016/j.jvolgeores.2004.10.012

Irvine, T.N.; Baragar, W.R. 1971. A guide to the chemical classification of the common volcanic rocks. Canadian Journal of Earth Sciences 8 (5): 523-548. https://doi.org/10.1139/e71-055

Kokelaar, P.; Busby, C. 1992. Subaqueous explosive eruption and welding of pyroclastic deposits. Science 257 (5067): 196-201. https://doi.org/10.1126/science.257.5067.196

McBirney, A.R. 1963. Factors governing the nature of submarine volcanism. Bulletin of Volcanology 26: 455-469. https://doi.org/10.1007/BF02597304

McPhie, J.; Doyle, M.; Allen, R. 1993. Volcanic Textures. A guide to the interpretation of textures in volcanic rocks. Centre for Ore Deposit and Exploration Studies, University of Tasmania: 198 p.

Middlemost, E.A.K. 1994. Naming materials in the magma/igneous rock system. Earth Science Reviews 37 (3-4): 215-224. https://doi.org/10.1016/0012-8252(94)90029-9

Moorhouse, B.L.; White, J.D.L. 2016. Interpreting ambiguous bedforms to distinguish subaerial base surge from subaqueous density current deposits. The Depositional Record 2 (2): 173-195. https://doi.org/10.1002/dep2.20

Newland, E.L.; Mingotti, N.; Woods, A.W. 2022. Dynamics of deep-submarine volcanic eruptions. Scientific Reports 12: 3276. https://doi.org/10.1038/s41598-022-07351-9

Niemeyer, H. 1989. El Complejo ígneo-sedimentario del Cordón de Lila, Región de Antofagasta: significado tectónico. Revista Geológica de Chile 16 (2): 163-181.

Niemeyer, H.; Götze, J.; Sanhueza, M.; Portilla, C. 2018. The Ordovician magmatic arc in the northern Chile-Argentina Andes between 21° and 26° south latitude. Journal of South American Earth Sciences 81: 204-214. https://doi.org/10.1016/j.jsames.2017.11.016

Pankhurst, R.J.; Hervé, F.; Fanning, C.M.; Calderón, M.; Niemeyer, H.; Griem-Klee, S.; Soto, F. 2016. The pre-Mesozoic rocks of northern Chile; U-Pb ages, and Hf and O isotopes. Earth-Science Reviews 152: 88-105. https://doi.org/10.1016/j.earscirev.2015.11.009

Pearce, J. 1996. Sources and settings of granitic rocks. Episodes 19 (4): 120-125. https://doi.org/10.18814/epiiugs/1996/v19i4/005

Pearce, J.A.; Harris, N.; Tindle, A.G. 1984. Trace element discrimination diagrams for the tectonic interpretation of granitic rocks. Journal of Petrology 25 (4): 956-983. https://doi.org/10.1093/petrology/25.4.956

Rapela, C.W.; Pankhurst, R.J.; Casquet, C.; Dahlquist, C.; Fanning, M.; Baldo, E.G.; Galindo, C.; Alasino, P.H.; Ramacciotti, C.D.; Verdecchia, S.O.; Murra, J.A.; Basei, M.A.S. 2018. A review of the Famatinian Ordovician magmatism in southern South America: Evidence of lithosphere reworking and continental subduction in the early proto-Andean margin of Gondwana. Earth-Science Reviews 187: 259-285. https://doi.org/10.1016/j.earscirev.2018.10.006

Shelley, D. 1992. Igneous and metamorphic rocks under the microscope. Chapman and Hall: 445 p. London.

Sparks, R.S.J.; Sirgurdsson, H.; Carey, S.N. 1980. The entrance of pyroclastic flows into the sea, II. Theoretical considerations on subaqueous emplacement and welding. Journal of Volcanology and Geothermal Research 7 (1-2): 97-105. https://doi.org/10.1016/0377-0273(80)90022-0

Stix, J. 1991. Subaqueous, intermediate to silicic-composition explosive volcanism: a review. Earth-Science Reviews 31 (1): 21-53. https://doi.org/10.1016/0012-8252(91)90041-D

White, J.D.L. 2000. Subaqueous eruption-fed density currents and their deposits. Precambrian Research 101 (2-4): 87-109. https://doi.org/10.1016/S0301-9268(99)00096-0

White, J.D.L.; Schipper, C.I.; Kano, K. 2015a. Submarine explosive eruptions. The Encyclopedia of Volcanoes (Second Edition): 553-569. https://doi.org/10.1016/B978-0-12-385938-9.00031-6

White, J.D.L.; McPhie, J.; Soule, S.A. 2015b. Submarine lavas and hyaloclastites. The Encyclopedia of Volcanoes (Second Edition): 363-375. https://doi.org/10.1016/B978-0-12-385938-9.00019-5

Wright, I.C.; Gamble, J.A.; Shane, P.A.R. 2003. Submarine silicic volcanism of the Healy caldera, southern Kermadek arc (SW Pacific): I - volcanology and eruption mechanisms. Bulletin of Volcanology 65: 15-29. https://doi.org/10.1007/s00445-002-0234-1

Zimmermann, U.; Niemeyer, H.; Meffre, S. 2010. Revealing the continental margin of Gondwana: the Ordovician arc of the Cordón de Lila (northern Chile). International Journal of Earth Sciences 99: 39-56. https://doi.org/10.1007/s00531-009-0483-8

Manuscript received: March 15, 2024; revised/accepted: July 30, 2024; available online: July 30, 2024.